Eur. Phys. J. D **6**, 407–413 (1999)

THE EUROPEAN PHYSICAL JOURNAL D
EDP Sciences

Spontaneous emission from a four-level Λ-V system

F. Plastina[a] and F. Piperno

Dipartimento di Fisica, Università della Calabria and Istituto Nazionale di Fisica della Materia, Unità di Cosenza
87036 Arcavacata di Rende (CS), Italy

Received: 20 October 1998

Abstract. We examine the decay dynamics of a free four-level system in the Λ-V configuration. Quantum interference strongly manifests itself in this system, as can be seen by looking at the combined spectral distribution of the two emitted photons and at the time evolution of the intermediate-level populations, whose effective lifetimes can become very long under certain conditions for the atomic parameters. This effect is attributable to a population transfer mechanism induced in the time evolution equations by the Fano terms, also responsible for the strong modifications of the spectral correlation between the emitted photons which we analyze in detail. Finally, population trapping can also occur when the two intermediate levels are degenerate.

PACS. 42.50.Ct Quantum description of interaction of light and matter; related experiments – 42.50.Gy Effects of atomic coherence on propagation, absorption, and amplification of light

1 Introduction

Quantum interference between different decay paths can lead to strong modifications of emission processes and spectra in multilevel atomic systems [1]. In the presence of initial atomic coherence among excited states, spectral line elimination and emission quenching or cancellation have been predicted for driven three- and four-level systems [2–4].

In some of these cases, a substantial part of population can remain trapped in the upper levels [5], its decay being prevented by destructive interference. All these phenomena have been described as a result of Fano-type interference because of their connection with the Fano effect involved in the interaction of a discrete state with a continuum or a quasi-continuum of levels [6]. It has also been recognized that this is a possible mechanism to produce optical amplification without population inversion [7,8].

Modifications of resonance fluorescence spectra have also been studied extensively [9] and strong narrowing of spectral lines have been predicted for driven three-level system in the V configuration [10]. The latter model has been the prototype for quantum interference studies because of the presence of two simultaneous transitions to a common ground state. If the two transition dipole moments are parallel, it shows peculiar interference effects also in the absence of coherent external driving field, as was noted by Zhu, Chan and Lee [11]. The interference-induced modifications in the emission spectrum reported in reference [11] are strictly related to the ones appearing in the spectral functions of the four-level system we examine in this paper, where we investigate the dynamics of a Λ-V configuration, with one upper, two intermediate and a lower state as shown in Figure 1. The presence of two possibilities of arriving at the ground state starting from the excited level can give rise to strong interference effects in the spectral correlation of the two emitted photons, which shows a dark minimum if the two lower transitions have parallel dipole moments. The evaluation of the combined spectral distribution of the two photons emitted when the system decays from $|a\rangle$ to $|c\rangle$ is the principal goal of the present work. Through the analysis of this function, which expresses intensity correlation in the frequency domain, we will show how the Fano mechanism can strongly alter the correlation between the emitted photons. In the absence of interference effect, indeed, this correlation merely expresses energy conservation, assuring the sum of the frequencies of the two photons to equal the frequency difference between the upper and lower atomic levels up to the spectral width of the first one. In the present case, instead, it also contains information about quantum interference and can be used as a tool to look at its effects. When the Fano terms are effective, indeed, emission cancellation and line narrowing are clearly reflected in the spectral photon correlation function, which becomes very small in the frequency range around which the quenching occurs.

We also analyze population dynamics, showing that the excited level occupation probability decreases with a time constant which strongly depends on interference. In particular, its value can become very large for small frequency separations between the two intermediate states.

[a] e-mail: plastina@fis.unical.it

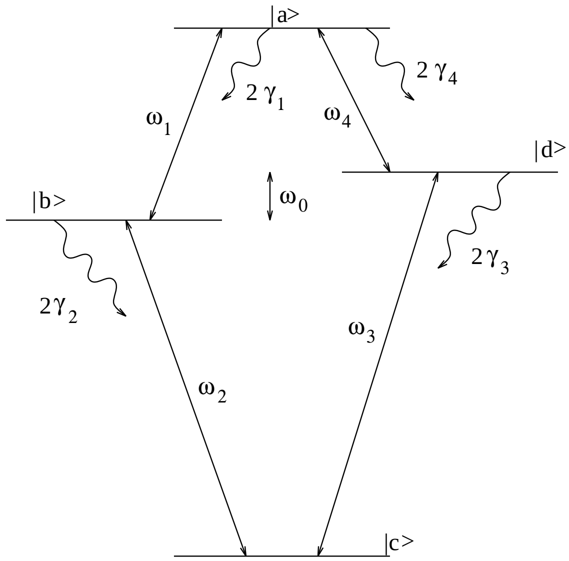

Fig. 1. Level scheme for a Λ-V system, the four transitions being enumerated in the anticlockwise direction, ω_i and $2\gamma_i$ are the frequency and decay constant for the i-th transition.

This can be also observed as strong narrowing of the spectral lines.

2 The model

Let us consider the system schematically represented in Figure 1 where definitions of transition frequencies and decay constants are also illustrated. Supposing the two upper transition frequencies to be substantially different from the lower ones, we separate the electromagnetic modes into two continua nearly resonant with the upper and lower transition and labelled with two indices, k and q, containing both wave vector and polarization information and referring to transitions $\{|a\rangle \to |b\rangle,\ |a\rangle \to |d\rangle\}$ and $\{|b\rangle \to |c\rangle,\ |d\rangle \to |c\rangle\}$, respectively.

The interaction picture Hamiltonian describing this system (written in the dipole and rotating wave approximations and with $\hbar = 1$) reads

$$H^{(i)} = i\sum_k \left\{ \left(g_k^{(1)} e^{i\delta_k^{(1)}t} |a\rangle\langle b| + g_k^{(4)} e^{i\delta_k^{(4)}t} |a\rangle\langle d| \right) a_k - \text{h.c.} \right\} + i\sum_q \left\{ \left(g_q^{(2)} e^{i\delta_q^{(2)}t} |b\rangle\langle c| + g_q^{(3)} e^{i\delta_q^{(3)}t} |d\rangle\langle c| \right) a_q - \text{h.c.} \right\}, \quad (1)$$

where

$$\delta_k^{(i)} = \omega_i - \omega_k\ ,\ i = 1, 4\,; \qquad \delta_q^{(l)} = \omega_l - \omega_q,\ l = 2, 3$$

are the vacuum modes detunings, a_k and a_q are the corresponding annihilation operators and

$$g_j^{(i)} = \sqrt{\frac{\omega_j}{2\varepsilon_0 V}}\, \boldsymbol{\varepsilon}_j \cdot \boldsymbol{d}_i \qquad i = 1, 2, 3, 4\,;\ j = k, q$$

are the dipole coupling constants, $\boldsymbol{\varepsilon}_j$ being the polarization unit vector for mode j and $\boldsymbol{d}_i$ the dipole moment for transition i. We will employ the usual Weisskopf-Wigner approach, supposing the system to be described by the state vector

$$|\psi, t\rangle = A(t)|a; \{0\}, \{0\}\rangle + \sum_k B_k(t)|b; 1_k, \{0\}\rangle + \sum_k D_k(t)|d; 1_k, \{0\}\rangle + \sum_k\sum_q C_{kq}|c; 1_k, 1_q\rangle \quad (2)$$

and choosing as initial condition

$$|\psi, 0\rangle = |a; \{0\}, \{0\}\rangle\ .$$

Projecting the Schrödinger equation over the basis states, we obtain the following set of equations for the coefficients:

$$\dot{A} = \sum_k \left(g_k^{(1)} e^{i\delta_k^{(1)}t} B_k + g_k^{(4)} e^{i\delta_k^{(4)}t} D_k \right)\,, \quad (3)$$

$$\dot{B}_k = -g_k^{(1)*} e^{-i\delta_k^{(1)}t} A + \sum_q g_q^{(2)} e^{i\delta_q^{(2)}} C_{kq}\,, \quad (4)$$

$$\dot{D}_k = -g_k^{(4)*} e^{-i\delta_k^{(4)}t} A + \sum_q g_q^{(3)} e^{i\delta_q^{(3)}} C_{kq}\,, \quad (5)$$

$$\dot{C}_{kq} = -g_q^{(2)*} e^{-i\delta_q^{(2)}t} B_k - g_q^{(3)*} e^{-i\delta_q^{(3)}t} D_k\,. \quad (6)$$

Using the formal solution of the latter in equations (4) and (5), performing the Weisskopf-Wigner approximation as in reference [11] and defining ω_0 as $\omega_0 = \omega_3 - \omega_2$, we get

$$\dot{B}_k \simeq -g_k^{(1)*} e^{-i\delta_k^{(1)}t} A - \gamma_2 B_k - p\sqrt{\gamma_2\,\gamma_3}\, e^{-i\omega_0 t} D_k\,, \quad (7)$$

$$\dot{D}_k \simeq -g_k^{(4)*} e^{-i\delta_k^{(4)}t} A - \gamma_3 D_k - p^*\sqrt{\gamma_2\,\gamma_3}\, e^{i\omega_0 t} B_k\,, \quad (8)$$

where $\gamma_i = \frac{2}{3}\frac{\omega_i^3\,|\boldsymbol{d}_i|^2}{4\pi\varepsilon_0 c^3}$ are the decay constants, while p is a parameter describing the alignment of the two lower transition dipole moments:

$$p = \frac{\boldsymbol{d}_2 \cdot \boldsymbol{d}_3^*}{|\boldsymbol{d}_2|\ |\boldsymbol{d}_3|}\ .$$

The key assumption for the validity of the approximation leading to equations (7) and (8) is that the frequency difference between the two intermediate levels has to be small: $\omega_0 \ll \omega_2, \omega_3$. We will assume ω_0 to be of the same order of magnitude as the decay constants because in this case the interference terms (proportional to $\sqrt{\gamma_2\,\gamma_3}$) strongly affect the time evolution of coefficients B_k and D_k. For larger ω_0, indeed, the last terms in equations (7) and (8) oscillate too rapidly and their contributions to the time evolution is negligible over the emission time scale. These terms describe an effective coupling between level $|b\rangle$ and $|d\rangle$ because of their simultaneous decay to the ground state *via* the same continuum of modes. The photons emitted during the $|b\rangle \to |c\rangle$ transition, for example, can be re-absorbed, bringing the system to level $|d\rangle$. This effective population transfer strongly modifies the time evolution of the intermediate-level populations. We will show that their decay is not simply governed by the

$$C_{kq}(\infty) = \frac{g_q^{(2)*} g_k^{(1)*}\left(i\delta_q^{(3)} + \gamma_3\right) + g_q^{(3)*} g_k^{(4)*}\left(i\delta_q^{(2)} + \gamma_2\right) - \sqrt{\gamma_2\,\gamma_3}\left(g_q^{(2)*} g_k^{(4)*} + g_k^{(1)*} g_q^{(3)*}\right)}{\{-i\left(\omega_q + \omega_k - \omega_{ac}\right) + \gamma_1 + \gamma_4\}\left\{\left[i(\omega_M - \omega_q) + \frac{\gamma_2 + \gamma_3}{2}\right]^2 + r^2\right\}} \tag{15}$$

rates γ_2 and γ_3, the probability of occupation of $|b\rangle$ and $|d\rangle$ decreasing to zero much more slowly.

In the following we will examine intermediate-level population dynamics and spectral functions supposing the dipole moments to be parallel, *i.e.* $p = 1$ ($p = -1$ would give us the same results because the parameter p enters the final expressions only through its modulus squared). The comparison between this case and the $p = 0$ one will clearly show the effects of Fano-like terms, the differences between the two situations being completely attributable to quantum interference.

2.1 Parallel dipole moments case

In this case, the formal solutions for B_k and D_k read

$$\begin{aligned}
B_k(t) &= e^{-i\frac{\omega_0}{2}t} \\
&\times \int_0^t \mathrm{d}t'\, e^{-\frac{\gamma_2+\gamma_3}{2}(t-t')}\left\{-f_4(t')\,\frac{\sqrt{\gamma_2\,\gamma_3}}{r}\sin r(t-t')\right. \\
&\left.+f_1(t')\left[\cos r(t-t') + \frac{i\omega_0 + \gamma_3 - \gamma_2}{2r}\sin r(t-t')\right]\right\},
\end{aligned} \tag{9}$$

$$\begin{aligned}
D_k(t) &= e^{i\frac{\omega_0}{2}t} \\
&\times \int_0^t \mathrm{d}t'\, e^{-\frac{\gamma_2+\gamma_3}{2}(t-t')}\left\{-f_1(t')\,\frac{\sqrt{\gamma_2\,\gamma_3}}{r}\sin r(t-t')\right. \\
&\left.+f_4(t')\left[\cos r(t-t') - \frac{i\omega_0 + \gamma_3 - \gamma_2}{2r}\sin r(t-t')\right]\right\},
\end{aligned} \tag{10}$$

having defined a complex frequency, r, by

$$r^2 = \frac{\omega_0^2 - (\gamma_2 + \gamma_3)^2 + 2i\omega_0(\gamma_2 - \gamma_3)}{4}\,, \tag{11}$$

and the two functions $f_i(t) = -g_k^{(i)*} e^{-i\delta_k^{(i)}t} A(t)$.

Inserting these solutions in equation (3) and using once again the Weisskopf-Wigner approximation, one obtains

$$\dot{A} \approx -(\gamma_1 + \gamma_4)A \longrightarrow A(t) = e^{-(\gamma_1+\gamma_4)t}\,. \tag{12}$$

This exponential behaviour could have been predicted from the beginning, but the analysis carried out until now allows us to easily obtain expressions for B_k and D_k:

$$\begin{aligned}
B_k(t) &= e^{-i\frac{\omega_0}{2}t} \\
&\times \left\{\left[-g_k^{(1)*}\left(\frac{1}{2} + \frac{\omega_0 - i(\gamma_3 - \gamma_2)}{4r}\right) - i g_k^{(4)*}\frac{\sqrt{\gamma_2\,\gamma_3}}{2r}\right]\right. \\
&\times \frac{e^{-[i(\omega_m - \omega_k) + \gamma_1 + \gamma_4]t} - e^{\left(ir - \frac{\gamma_2+\gamma_3}{2}\right)t}}{-i\left(\omega_m - \omega_k + r\right) + \frac{\gamma_2 + \gamma_3}{2} - (\gamma_1 + \gamma_4)} \\
&\left. + \text{the same with } r \to -r\right\},
\end{aligned} \tag{13}$$

$$\begin{aligned}
D_k(t) &= e^{i\frac{\omega_0}{2}t} \\
&\times \left\{\left[-g_k^{(4)*}\left(\frac{1}{2} - \frac{\omega_0 - i(\gamma_3 - \gamma_2)}{4r}\right) - i g_k^{(1)*}\frac{\sqrt{\gamma_2\,\gamma_3}}{2r}\right]\right. \\
&\times \frac{e^{-[i(\omega_m - \omega_k) + \gamma_1 + \gamma_4]t} - e^{\left(ir - \frac{\gamma_2+\gamma_3}{2}\right)t}}{-i\left(\omega_m - \omega_k + r\right) + \frac{\gamma_2 + \gamma_3}{2} - (\gamma_1 + \gamma_4)} \\
&\left. + \text{the same with } r \to -r\right\},
\end{aligned} \tag{14}$$

where we have defined ω_m as: $\omega_m = \frac{\omega_1 + \omega_4}{2}$.

From these relations and using equation (6), we can easily obtain $C_{kq}(t)$ by direct integration:

$$\begin{aligned}
C_{kq}(t) = &-g_q^{(2)*}\int_0^t \mathrm{d}t'\, e^{-i\delta_q^{(2)}t'} B_k(t') \\
&-g_q^{(3)*}\int_0^t \mathrm{d}t'\, e^{-i\delta_q^{(3)}t'} D_k(t')\,.
\end{aligned}$$

Its expression, however, is very long and not easily readable. We report the long-time behaviour only:

see equation (15) above

having defined ω_M as the mid-frequency between ω_2 and ω_3, so that $\omega_M = \omega_{ac} - \omega_m$. This expression will be used in the following to obtain the spectral functions.

2.2 Case of orthogonal dipole moments

For the sake of completeness and for future reference, we report the same quantities obtained above, also for the $p = 0$ case. When the dipole moments are mutually orthogonal, the system can be regarded as a pair of decoupled three-level systems in cascade configuration. The relations expressed in (12) are still valid, so the upper level population decreases exponentially. For $B_k(t)$ and $D_k(t)$ we obtain

$$B_k(t) = -g_k^{(1)*} \frac{e^{-\left[i\delta_k^{(1)}+(\gamma_1+\gamma_4)\right]t} - e^{-\gamma_2 t}}{-i\delta_k^{(1)} - (\gamma_1+\gamma_4) + \gamma_2}, \qquad (16)$$

$$D_k(t) = -g_k^{(4)*} \frac{e^{-\left[i\delta_k^{(4)}+(\gamma_1+\gamma_4)\right]t} - e^{-\gamma_3 t}}{-i\delta_k^{(4)} - (\gamma_1+\gamma_4) + \gamma_3}. \qquad (17)$$

Once again, C_{kq} is easily calculated by means of equation (6). Its long-time behaviour is given by

$$C_{kq}(\infty) = \frac{1}{i\left(\omega_k+\omega_q-\omega_{ac}\right) - (\gamma_1+\gamma_4)} \times \left\{ \frac{g_k^{(1)*} g_q^{(2)*}}{i(\omega_q-\omega_2) - \gamma_2} + \frac{g_k^{(4)*} g_q^{(3)*}}{i(\omega_q-\omega_3) - \gamma_3} \right\}. \qquad (18)$$

3 Evolution of population

The probability of occupation of levels $|b\rangle$ and $|d\rangle$ can be obtained as

$$\rho_{bb}(t) = \sum_k |B_k(t)|^2, \qquad \rho_{dd}(t) = \sum_k |D_k(t)|^2.$$

The calculations involved are rather cumbersome; some conclusions, however, can be drawn before the explicit evaluation of these expressions. It is easy to show that, when $\omega_0 \neq 0$, the imaginary part of r is always smaller than $\frac{\gamma_2+\gamma_3}{2}$, so that

$$\lim_{t\to\infty} \rho_{bb}(t) = \lim_{t\to\infty} \rho_{dd}(t) = 0.$$

On the other hand, when the two intermediate levels are degenerate, we have

$$r = i\frac{\gamma_2+\gamma_3}{2}$$

and one can expect some population to remain trapped in $|b\rangle$ or $|d\rangle$. This result should have been expected in view of the analysis of reference [11].

Even if the system finally decays to level $|c\rangle$, when $\omega_0 \neq 0$ the time evolution of ρ_{bb} and ρ_{dd} is greatly affected by the coupling between B_k and D_k expressed in equations (7) and (8). The greatest difference between the $p = 1$ and the $p = 0$ cases, as one can see from Figure 2, is that, after a first period in which ρ_{bb} increases because of the transition from the upper level, in the former the probability of occupation of $|b\rangle$ decays very slowly in time (the lower ω_0, the slower the decay, whose time constant is approximately given by the inverse of $(\gamma_2+\gamma_3) - 2\mathrm{Im}\{r\}$ and can reach a value very close to zero if ω_0 is smaller or at least of the order of the decay constants), while in the latter the decay is purely exponential with a time constant approximately given by $\frac{1}{\gamma_2}$.

When $\gamma_2 = \gamma_3$, as is the case in the figure, r can be purely real or purely imaginary depending on whether

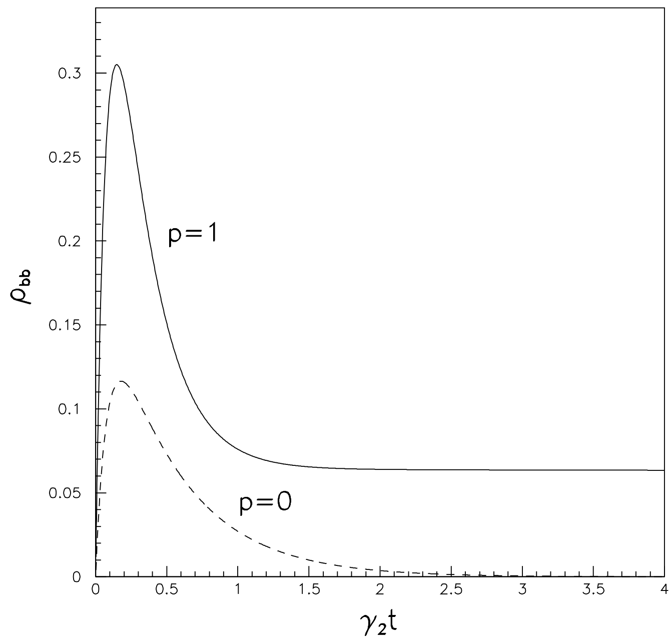

Fig. 2. Evolution of the population of level $|b\rangle$, plotted *versus* time measured in units of $\frac{1}{\gamma_2}$, with $\gamma_1 = \gamma_2 = \gamma_3$, $\gamma_4 = 5\gamma_2$ and $\omega_0 = 0.1\gamma_2$.

$\omega_0 > 2\gamma_2$ or not. If this inequality holds, interference between the two transitions becomes fairly feeble and the evolution of ρ_{bb} is almost the same with both $p = 1$ and $p = 0$. On the contrary, when the inequality does not hold, the lifetimes of the intermediate levels can become much longer than $\frac{1}{\gamma_2}$, also causing a strong narrowing of one of the peak in the lower transition spectrum (see next Section).

As already mentioned, a completely different time evolution occurs if the intermediate levels are degenerate. In this case, indeed, ρ_{bb} and ρ_{dd} can reach stationary values different from zero, given by

$$\lim_{t\to\infty} \rho_{bb}(t) = \frac{\gamma_3}{(\gamma_2+\gamma_3)^2} \frac{\left(\sqrt{\gamma_1\gamma_3} - \sqrt{\gamma_2\gamma_4}\right)^2}{\gamma_1+\gamma_4}, \qquad (19)$$

$$\lim_{t\to\infty} \rho_{dd}(t) = \frac{\gamma_2}{(\gamma_2+\gamma_3)^2} \frac{\left(\sqrt{\gamma_1\gamma_3} - \sqrt{\gamma_2\gamma_4}\right)^2}{\gamma_1+\gamma_4}. \qquad (20)$$

Thus, a population trapping is present, which has no counterpart in the $p = 0$ case. This happens because, in this case, the two transition dipole moments $\boldsymbol{d}_2$ and $\boldsymbol{d}_3$ oscillate with the same frequency but with a phase shift of π, thus interfering destructively and preventing the emission of the second photon and trapping the atomic population in an excited state. As will be shown in the next section, a minor destructive interference effect is still present when ω_0 is different from zero (but still not so large with respect to γ_2 and γ_3) causing a substantial quenching of the emission probability in a limited frequency range.

4 Spectral functions

Two spectral distributions have to be calculated to characterize the radiation spontaneously emitted by the atom, one for the upper and another for the lower transition photons.

These two functions can be obtained by direct integration from the so-called combined spectral distribution [12], which, going to the continuum of electromagnetic modes, has the expression

$$S(\omega_k,\omega_q) = \sum_{\lambda_k}\int \mathrm{d}^2\Omega_k\,\frac{\omega_k^2}{c^3}\sum_{\lambda_q}\int \mathrm{d}^2\Omega_q\,\frac{\omega_q^2}{c^3}\left|C_{\vec{k}\,\lambda_k,\vec{q}\,\lambda_q}(\infty)\right|^2 \quad (21)$$

integrations being performed over the wave vector directions.

The spectral distributions of radiation emitted during the two independent steps that bring the system from $|a\rangle$ to $|c\rangle$, $S_{\rm up}(\omega_k)$ and $S_{\rm down}(\omega_q)$, can be found by integration of the combined distribution over the other frequency.

Using the results (18) and (15) for the $p=0$ and $p=1$ cases, respectively, we find

$$S(\omega_k,\omega_q) = \frac{1}{\pi^2\left\{(\omega_k+\omega_q-\omega_{ac})^2+(\gamma_1+\gamma_4)^2\right\}} \times\left\{\frac{\gamma_1\gamma_2}{(\omega_q-\omega_2)^2+\gamma_2^2}+\frac{\gamma_3\gamma_4}{(\omega_q-\omega_3)^2+\gamma_3^2}\right\}, \quad \text{if } p=0\,, \quad (22)$$

$$S(\omega_k,\omega_q) = \frac{1}{\pi^2\left\{(\omega_k+\omega_q-\omega_{ac})^2+(\gamma_1+\gamma_4)^2\right\}} \times\frac{\left[\sqrt{\gamma_1\,\gamma_2}\delta_q^{(3)}+\sqrt{\gamma_3\,\gamma_4}\delta_q^{(2)}\right]^2}{\left(\delta_q^{(2)}\delta_q^{(3)}\right)^2+\left(\gamma_2\delta_q^{(3)}+\gamma_3\delta_q^{(2)}\right)^2}, \quad \text{if } p=1\,, \quad (23)$$

where, in the $p=1$ case, we have used the fact that the upper transitions dipole moments should also be parallel, as was already noted in reference [5]. Apart from the common first factor which ensures energy conservation within the width of the upper level, these two functions have a completely different structure, see Figures 3 and 4. The first one is a sum of two bi-dimensional Lorentzians, while the second one is not simply a sum of functions with two different peaks because of the presence of an interference term. This interference term, as one can see by comparing the two plots, gives rise to a strong quenching in the region between the two peaks, and to a narrowing of the left maximum in the $\omega_q-\omega_M$ direction.

The origin of these very different behaviours lies in the above introduced population transfer mechanism due to the Fano terms in equations (7) and (8). We can understand that, when $p=0$, the second transition has already been selected after the first emission: if the atom decays

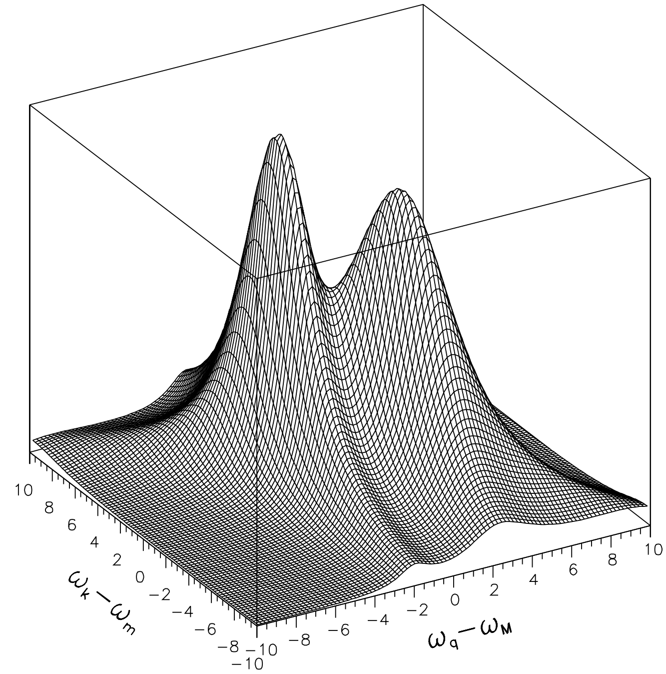

Fig. 3. The combined spectral distribution function expressing the spectral photon correlation in the $p=0$ case, equation (22), with $\gamma_1=\gamma_2=1$, $\gamma_3=\gamma_4=2$, $\omega_0=4$.

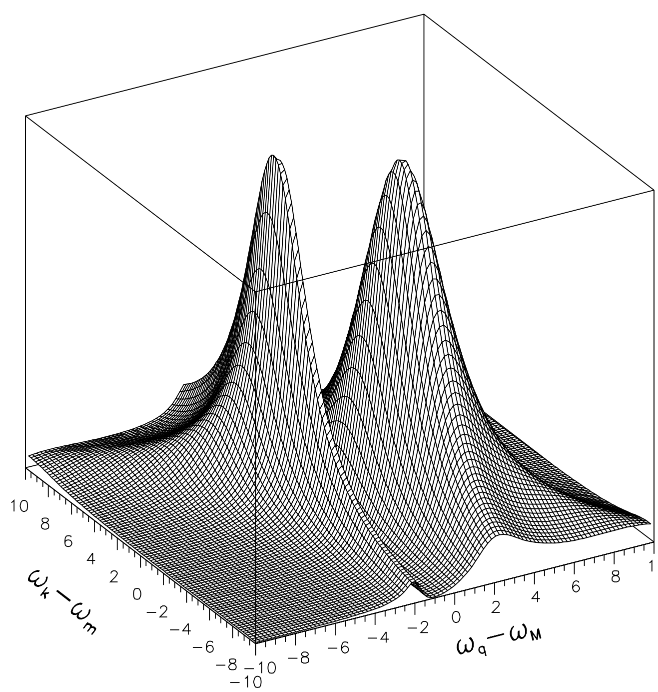

Fig. 4. $S(\omega_k,\omega_q)$ in the $p=1$ case, equation (23), with the same parameter values as in Figure 3.

from $|a\rangle$ to $|b\rangle$ (or $|d\rangle$), then in the second step it will produce radiation with a Lorentzian spectral profile centered at the frequency ω_2 (ω_3).

When $p=1$, on the other hand, the second photon is not so strongly correlated with the first. Even if the first transition brings the system to level $|b\rangle$, the second photon can still come out from the $|d\rangle \to |c\rangle$ transition, because of the possibility of the atomic population to undergo a transition from $|b\rangle$ to $|d\rangle$ via the virtual emission and reabsorption processes induced by the Fano interference.

It is impossible to say "which path" the atom has followed to decay from $|a\rangle$ to $|c\rangle$ and it is just the interference between the two interfering paths that produces the modifications observed in the spectral photon correlation function.

Because of its numerator, the combined distribution function of equation (23) has a zero for

$$\omega_q = \frac{\sqrt{\gamma_1\,\gamma_2}\,\omega_3 + \sqrt{\gamma_3\,\gamma_4}\,\omega_2}{\sqrt{\gamma_1\,\gamma_2} + \sqrt{\gamma_3\,\gamma_4}},$$

meaning that, during the second transition from $|b\rangle$ or $|d\rangle$ to the ground state, the system has a zero probability of emitting photons of this frequency. This can also be seen very clearly in the lower transitions spectrum which shows a dark minimum at this point.

Indeed, $S_{\rm down}(\omega_q)$ also provides a tool for the comparison between the two cases. It can be evaluated straightforwardly, giving

$$S_{\rm down}(\omega_q) \propto \frac{1}{\gamma_1+\gamma_4} \times \left\{ \frac{\gamma_1\gamma_2}{(\omega_q-\omega_2)^2+\gamma_2^2} + \frac{\gamma_3\gamma_4}{(\omega_q-\omega_3)^2+\gamma_3^2} \right\}, \quad \text{if } p=0, \tag{24}$$

and

$$S_{\rm down}(\omega_q) \propto \frac{1}{\gamma_1+\gamma_4} \times \frac{\left[\sqrt{\gamma_1\,\gamma_2}\,(\omega_q-\omega_3)+\sqrt{\gamma_3\,\gamma_4}\,(\omega_q-\omega_2)\right]^2}{\left\{(\omega_q-\omega_M)^2-\frac{\omega_0^2}{4}\right\}^2+\{\gamma_2\,(\omega_q-\omega_3)+\gamma_3\,(\omega_q-\omega_2)\}^2}, \quad \text{if } p=1. \tag{25}$$

While the first of the two functions is a sum of two Lorentzians, with maxima at the two transition frequencies and widths given by their natural values, the second one shows strong modifications, see Figure 5. Apart from the zero, whose presence was already pointed out, interference can give rise to a strong narrowing of one of the lines and to an emission quenching, provided that the decay constants and transition frequencies have suitable values. In particular, in Figure 6, we plotted the spectral function with a very small value of ω_0 and with γ_1 much different from γ_4, thus supposing the transition rate from level $|a\rangle$ to $|b\rangle$ to be significantly greater than that from $|a\rangle$ to $|d\rangle$. As one can see, one of the peaks disappears in the $p=0$ case; because of its small height, it is indistinguishable from the tail of the other Lorentzian. In the $p=1$ case, on the other hand, we see a large increase and narrowing of the maximum roughly corresponding to the $|b\rangle$ to $|c\rangle$ transition, and a substantial quenching of the second maximum. The lifetime of level $|b\rangle$, in this situation, becomes very large because, through the transfer mechanism already mentioned, some population from $|d\rangle$ can reach the other intermediate level at times much longer than $\frac{1}{\gamma_1}$ which would be the typical time for population arrival from $|a\rangle$ in the absence of interference effects. Furthermore, as was noted in the previous section, ρ_{bb} decays very slowly in this case, because of the smallness of ω_0 with respect to $(\gamma_1+\gamma_2)$. The overall line shape can be

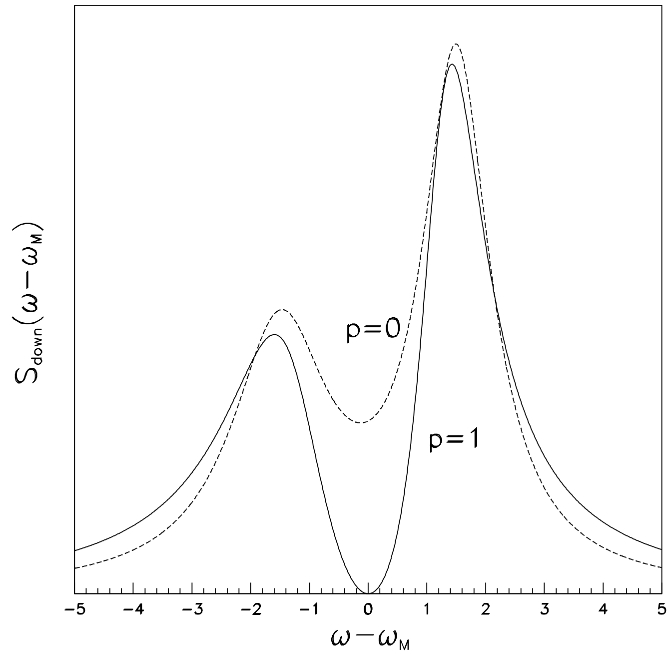

Fig. 5. Spectral distribution of lower transitions photons in the $p=1$ and $p=0$ cases, with $\gamma_1=\gamma_3=0.7$, $\gamma_2=\gamma_4=1$, $\omega_0=3$.

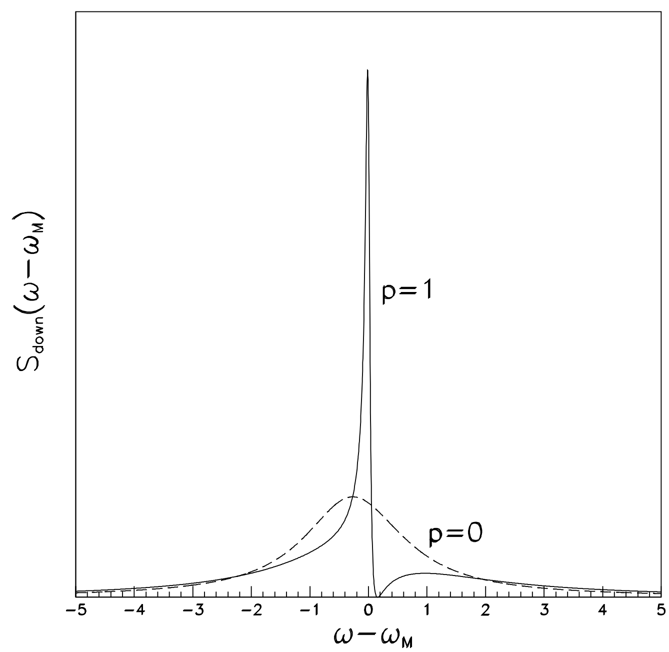

Fig. 6. The same as Figure 5, with $\gamma_1=\gamma_2=\gamma_3=1$, $\gamma_4=0.1$, $\omega_0=0.6$.

thought as a result of constructive interference, giving rise to the substantial intensity increase observed in Figure 6. The zero, on the other hand, results from destructive interference between the two decay amplitudes for transitions $|b\rangle \to |c\rangle$ and $|d\rangle \to |c\rangle$. At the frequency of the dark minimum, actually, they have equal magnitude but are exactly out of phase.

5 Conclusions

We have shown how quantum interference affects the decay dynamics of a free four-level system in the Λ-V configuration. The possibility of decaying to the same continuum of states provides an effective coupling between the two intermediate levels producing a population transfer mechanism which strongly modifies the decay rates. For suitable parameter values the effective lifetime of one of these levels can be substantially altered with respect to its natural value, resulting in a strong line narrowing in the spontaneous emission spectrum. The lifetime of the intermediate levels increases more and more as the frequency difference between them goes to zero, a true population trapping occurring when they are degenerate. Besides these manifestations, destructive interference is also present, which causes spontaneous emission quenching, the combined spectral distribution of the two emitted photons showing a dark minimum in the region between the two lower transition frequencies. Both the quenching and narrowing phenomena are clearly displayed by the combined spectral distribution function and we can conclude that the analysis of the intensity correlation in the spectral domain can be a useful tool to investigate quantum interference manifestations. In the present case, they are easily attributable to the presence of Fano-like terms in the equations for the state vector coefficients. These terms, in turn, are due, physically, to the indistinguishability of the lower transitions photons, which allows for the possibility of reabsorption after a first transition to the ground state and which is granted when the two transition dipole moments are parallel and the frequency difference between the two intermediate levels is of the same order as the decay constants. This explains why both conditions are required to obtain strong interference effects.

References

1. For a recent review, see E. Arimondo in *Progress in Optics XXXV*, edited by E. Wolf (Elsevier, Amsterdam, 1996) p. 257.
2. P.R. Fontana, R.P. Srivastava, Phys. Rev. A **7**, 1866 (1973); M.O. Scully, S.Y. Zhu, A. Gavrielides, Phys. Rev. Lett. **62**, 2813, (1989); S.Y. Zhu, L.M. Narducci, M.O. Scully, Phys. Rev. A **52**, 4791 (1995); F. Plastina, F. Piperno, unpublished.
3. S.Y. Zhu, M.O. Scully, Phys. Rev. Lett. **76**, 388 (1996); H.R. Xia, C.Y. Ye, S.Y. Zhu, Phys. Rev. Lett. **76**, 1032 (1996); G.S. Agarwal, Phys. Rev. A **55**, 2457 (1997); H. Lee, P. Polynkin, M.O. Scully, S.Y. Zhu, Phys. Rev. A **55**, 4454 (1997).
4. G.S. Agarwal, Phys. Rev. A **54**, 3735 (1996).
5. H. Huang, S.Y. Zhu, M.S. Zubairy, Phys. Rev. A **55**, 744 (1997).
6. U. Fano, Phys. Rev. **124**, 1866 (1961); D. Agassi, Phys. Rev. A **30**, 2449 (1984); D. Agassi, J.H. Eberly, Phys. Rev. A **334**, 2843 (1986); S. Tarzi, P.M. Radmore, Phys. Rev. A **37**, 4734 (1988); P.L. Knight, M.A. Lauder, B.J. Dalton, Phys. Rep. **190**, 1 (1990).
7. S.E. Harris, Phys. Rev. Lett. **62**, 1033 (1989); O. Kocharovskaya, P. Mandel, Phys. Rev. A **42**, 523 (1990); A. Imamoglu, J.E. Field, S.E. Harris, Phys. Rev. Lett. **66**, 1154 (1991); C. Keitel, O. Kocharovskaya, L.M. Narducci, M.O. Scully, S.Y. Zhu, Phys. Rev. A **48**, 3196 (1993).
8. O. Kocharovskaya, Phys. Rep. **219**, 175 (1992); M. Fleischhauer, T. McIllrath, M.O. Scully, Appl. Phys. B **66**, S123 (1995); G. Grynberg, M. Pinard, P. Mandel, Phys. Rev. A **54**, 776 (1996); J.L. Cohen, P.R. Berman, Phys. Rev. A **55**, 3900 (1997).
9. D.A. Cardimona, M.G. Raymer, C.R. Stroud jr, J. Phys. B **12**, 55 (1982); L.M. Narducci, M.O. Scully, G.L. Oppo, P. Ru, J. Tredicce, Phys. Rev. A **42**, 1630 (1990); A.S. Manka, H.M. Doss, L.M. Narducci, P. Ru, G.L. Oppo, Phys. Rev. A **43**, 3748 (1991); D.J. Gauthier, Y.F. Zhu, T.W. Mossberg, Phys. Rev. Lett. **66**, 2460 (1991).
10. P. Zhou, S. Swain, Phys. Rev. Lett. **77**, 3995 (1996); P. Zhou, S. Swain, Phys. Rev. A **56**, 3011 (1997).
11. S.Y. Zhu, R.C.F. Chan, C.P. Lee, Phys. Rev. A **52**, 710 (1995); see also S.Y. Zhu, M.O. Scully, reference [3].
12. See, for example, C. Cohen-Tannoudji, J. Dupont-Roc, G. Grynberg, *Atom-Photon Interaction, Basic Processes and Applications* (Wiley, New York, 1992).